Accuracy of ANN Based Methodology for Load Composition Forecasting at Bulk Supply Buses

Yizheng Xu, *Graduate Student Member, IEEE,* and Jovica.V. Milanović, *Fellow, IEEE*
University of Manchester, Manchester, UK
yizheng.xu@postgrad.manchester.ac.uk; milanovic@manchester.ac.uk

***Abstract*— Accurate prediction of load composition at bulk supply points can significantly improve power system planning, electricity market analysis and demand side management. This paper discusses an artificial neural network (ANN) based approach to forecasting load composition at the bulk supply bus based on RMS measurement of voltage, real and reactive power and local forecasted weather. Probabilistic distributions and confidence levels of the prediction under different prediction error intervals have been derived and analysed. It is demonstrated that the approach yields prediction of load composition with errors typically less than 10%.**

***Index Terms*— Black box system, confidence level, Monte Carlo, load disaggregation, load forecasting**

I. INTRODUCTION

Because of the daily and seasonally variation of the demand associated with end-users' consumption habits, the load composition at a bulk supply point frequently changes. The accurate prediction of total demand offers great saving potential for power system planning and investment activity. Forecasting of load composition will not only achieve the above objectives, but also facilitate more effective demand side management (DSM) and integration of renewable energy sources (RES). Therefore, being able to predict load composition accurately helps with making effective DSM and RES integration decisions close to real time, and this contributes to the secure, stable and economic operation of the whole power system.

Significant effort has been put in the past into both total demand forecasting and load disaggregation. Artificial intelligence (AI) tools such as artificial neural networks (ANN) and (adaptive neural) fuzzy inference systems (FIS) have been widely applied to both real power forecasting [1, 2] and reactive power forecasting [3, 4] and have demonstrated high accuracy. As far as load disaggregation is concerned, intrusive load monitoring [5] and non-intrusive load monitoring [6, 7] were the most widely used approaches. The former spends a significant amount of time and expense on customer surveys, installation of metering devices, data classification and processing etc., which makes the output a 'historical data library of specific customers in specific areas for reference only'. Besides, the accuracy of the customer surveys is difficult to be ensured for a number of reasons including missing or incomplete data and vague customer recording. Non-intrusive load monitoring can achieve very high accuracy, but requires relatively high monitoring resolution (faster than 1Hz) of load signature [8, 9] measurements at the supply point, which are not achievable under most circumstances. Therefore, more practical and robust methodologies are needed for load disaggregation (dividing load composition in particular) requiring less data processing time and relaying on available measurement data.

This paper proposes an Artificial Neural Network (ANN) based framework for forecasting load composition at given bulk supply bus based on general substation measurements of RMS voltage (V), real (P) and reactive (Q) power and local forecasted weather information (i.e. temperature, humidity, wind speed etc.). The "black box" forecasting system consists of two forecasting black boxes (one for P and the other for Q) and one disaggregation black box. The output of the black box forecasting system is the forecasted percentage of load composition at given bus. As the total load forecasting approach and the disaggregation approach are developed separately, they are considered independent of each other. In the disaggregation approach, Monte Carlo Simulation is used to generate the training and validation data. The confidence levels of load composition forecasting under different prediction error intervals are analysed. The forecasting approach is implemented in MATLAB 2011a on an Intel(R) Core (TM) i5-2400 CPU @ 3.10GHz computer installed with 32-bit Windows XP system.

II. ARTIFICIAL NEURAL NETWORK

A two-layer feed-forward (FF) ANN, shown in Fig.1, is employed in this study because of its simple structure and potential ability to represent almost all input-output relationships with a finite number of discontinuities, as long as an appropriate size is assigned to the hidden layer [10]. Either of the two layers contains an input vector $\boldsymbol{p}$, a weight matrix $\boldsymbol{W}$, a bias vector $\boldsymbol{b}$, a sum operator, a transfer function f and an output vector $\boldsymbol{a}$. The relationship between the input and the output in either layer can be represented by (1). Further theoretical background about ANN operation mechanism is described in [10, 11].

This research is partly funded by the EPSRC project Autonomic Power Systems and partly by EU FP7 project SuSTAINABLE

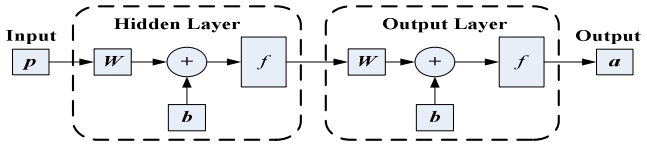

Fig. 1 Structure of a feed-forward ANN

$$\boldsymbol{a} = f(\boldsymbol{W}^T\boldsymbol{p} + \boldsymbol{b}) \quad (1)$$

III. Overview of the "Black Box" Forecasting System

The black box system proposed for load composition forecasting approaches is shown in Fig.2. The system contains two total demand forecasting boxes (Box 1 for P forecasting and Box 2 for Q forecasting) and one load disaggregation box (Box 3). It first predicts the future total demand at the bus and then disaggregates the forecasted demand into possible load compositions. The inputs of the whole system are RMS P and Q measurements at the bulk supply point and the local forecasted weather data, and the outputs are the forecasted percentage of the load compositions at the bulk supply point.

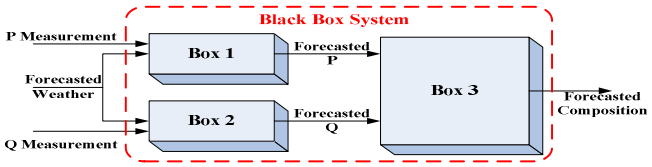

Fig. 2. Black box system and its inputs and outputs

IV. Total Load Forecasting Approach

The AI-based total demand forecasting approach includes a training process and a validation process. As the approach for both P and Q forecasting has been introduced in [1, 3, 4], in this paper, only data collection, ANN parameter configuration and training algorithm selection are discussed in details.

For simplicity of comparison, all demand curves are normalized to per unit value by dividing the actual value by the peak P demand. In [1, 3, 4], demands of previous days are chosen as the input for ANN training, which induces obvious forecasting errors when the dates transfer from weekdays to weekends and vice versa. To reduce such errors, one of the ANN inputs for training in this study is selected as the normalized historical average daily demand curve (NHADDC) of either the weekday or the weekend, dependent on the type of the forecasting day. NHADDC is obtained by normalizing each collected historical daily demand curve to the corresponding daily peak P demand and then taking the arithmetic average of the normalized demand data at every sampling time during the day. The P and Q demand data in this study are collected every 30 *min* from substations by local distribution company which contains 48 samples per day. Another ANN input is every 30 min collected weather data (temperature in °C, humidity in p.u, wind speed in km/h etc.) on the forecasting day, collected from Weather.Org and posted on [12]. The ANN target is every 30 min normalized demand curve data on the forecasting day. As the final output (the predicted demand) lies within the range [0,1], log-sigmoid (*logsig*) and tan-sigmoid (*tansig*) are selected as the transfer function [10] of the hidden layer and the output layer of ANN respectively, and Bayesian Regulation Backpropagation (BRBP) is selected as the ANN training algorithm [10] for its high accuracy and robustness. The relationship between the input and the target is saved in the ANN for validation and further use.

A similar data collection procedure as described in the training process is implemented for the validation process. The inputs are the same NHADDC as described in the training process and every 30*min* weather data on new forecasting days. By injecting the inputs to the trained ANN, it will produce outputs (i.e. the forecasted demand), and the outputs will be compared with the targets (i.e. the actual demand on new forecasted days). The absolute error between the forecasted demand and the actual demand is adopted for assessing forecasting accuracy.

As P and Q are considered equally important to load disaggregation introduced in later sections, in this study, the overall total load forecasting error is defined as the arithmetic average value of the absolute P prediction error and the absolute Q prediction error [13]. Due to the large amount of data involved in the validation process, probability density function (PDF) and cumulative distribution function (CDF) of the overall total load forecasting error are used. They are denoted as $f_F(e_F)$ and $F_F(e_F)$ respectively. The probabilistic approach helps assessing the uncertainty associated with total load forecasting and facilitates calculation of confidence levels in load composition forecasting.

V. Disaggregation Approach

The disaggregation approach is independent of the total load forecasting approach and vice versa. Therefore, the disaggregation black box is developed and tested offline with thousands of randomly generated datasets which cover almost all possible combinations of load composition. Once tested successfully, it is integrated with the total load forecasting boxes. The disaggregation approach makes use of voltage dependent load models [14].

A. Load Modeling

1) Most Commonly Used Static Load Models

Voltage-dependent load models are adopted in the disaggregation approach to obtain the relationships between load compositions and P&Q&V measurements. Because the methodology developed in this study is based on the every 30 min or 60 min steady state RMS P&Q&V measurements at the bus, only static load models are discussed; the dynamic characteristics of P and Q responses (i.e. the transient processes in seconds) [15] are not considered in this study because of its shorter timeframe. The most commonly used types of voltage dependent load models are ZIP model [15], exponential load model shown as (2), and general polynomial model shown as (3), where P and Q represents the real and reactive power of the load, P_0 and Q_0 are the initial real and reactive power, V and V_0 are the actual and initial load supply voltage, α and β are exponential model coefficients for real and reactive power, *Para* represents other parameters apart from V (i.e. inductance, capacitance, base power etc.), and f represents a V and *Para* dependent function.

$$P = P_0 \left(\frac{V}{V_0}\right)^{\alpha} \text{ and } Q = Q_0 \left(\frac{V}{V_0}\right)^{\beta} \quad (2)$$

$$P = f_P(V, Para) \text{ and } Q = f_Q(V, Para) \quad (3)$$

Generally, the exponential model coefficients are much more voltage-dependent than ZIP model coefficients and general polynomial model coefficients [15], and the load modelling result presented in [16] also shows that under most circumstances, an exponential load model with constant coefficient performs less accurately than a ZIP or polynomial model within the same voltage range. However, exponential load mode still gains preferences in most case studies because of its convenience and simplicity, as long as the relationship between the exponent and the voltage can be obtained.

2) Voltage-dependent Exponential Model Coefficient

To simplify the programming process and to demonstrate the approach, the exponential load model is adopted in this study. The value of exponents α and β under different voltages can be calculated from (2) ideally with adequate real measured data of V, P and Q. If field measurement data are not available, estimates of P and Q calculated with the more accurate polynomial or ZIP models [16] can be adopted to replace the real measured data. The relationship between P exponent α and V in both cases are shown in (4): the first equation if measured data is available, and the second if it is not, where $\alpha(V)$ is exponential model coefficient for P under Voltage V, $P_{measurement}$ is field measurement data of P, and other parameters have the same definitions as in (2) and (3). A similar relationship applies to Q exponent $\beta(V)$.

$$\alpha(V) = \frac{ln\left(\frac{P_{measurement}}{P_0}\right)}{ln\left(\frac{V}{V_0}\right)} \text{ or } \alpha(V) = \frac{ln\left[\frac{f_P(V,Para)}{P_0}\right]}{ln\left(\frac{V}{V_0}\right)} \quad (4)$$

According to the basic theory of the component-based load modelling approach introduced in [15], loads are classified into different load categories based on their load characteristics. In this study, loads are classified into eight categories [16-19], including: 1) lighting (L); 2) SMPS (switch mode power supply); 3) rectifier (REC); 4) residential cold load (RCL); 5) residential wet load (RWL); 6) resistive load (R); 7) 3-phase constant torque induction motors (CTIM3); 8) 3-phase quadratic torque induction motors (QTIM3). Category 7) and 8) are widely distributed in commercial and industrial load sectors. The ZIP models (or the polynomial models) used in this study to derive the exponent-voltage relationship for different load categories are illustrated, validated and recommended by measurement-based approach load modelling in [16-19].

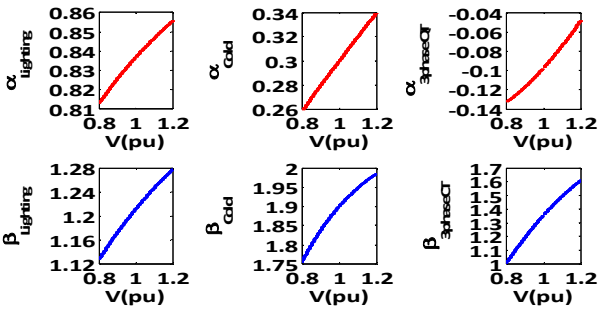

Fig. 3. P&Q exponent-voltage relationship of different load categories

Exponent-voltage relationship plots of lighting, RCL, and CTIM3 are shown in Fig.3. Exponent-voltage relationships of other load categories are not shown in the paper due to space limitation. Once obtained, the relationships are stored in either ANNs or mathematical formula for further use. With these relationships, actual P and Q for individual load categories under different voltage can be calculated using (2).

3) Aggregate Load Models

If the composition of each load category is known, via component-based load modelling approach, the aggregate load at the bulk supply point can be represented by (5), where P_{Agg} and Q_{Agg} are aggregate load P and Q consumption in per unit, N is the total number of load categories, w_i is the weighting factor of load category i, P_i and Q_i are actual P and Q consumption of load category i in per unit. Weighting factor here is defined as the percentage of each different load category participating in the bulk supply point. This relationship will be used in the load disaggregation described in following sections to generate the ANN input and the target.

$$P_{Agg} = \sum_{i=1}^{N} w_i P_i \text{ and } Q_{Agg} = \sum_{i=1}^{N} w_i Q_i \quad (5)$$

B. Disaggregation

The disaggregation approach can be summarized as follows: i) generate random voltages and weighting factors for training, and derive all combinations of voltages and weighting factors; ii) use the result from i) and Equation (2), (4) and (5) to define the input (P&Q&V) and the target (weighting factors) for ANN; iii) train ANN and save trained ANN; iv) remove voltage in ii), repeat iii); v) repeat i) to generate data for validation; vi) validation using saved network in both iii) and iv) and compare the two cases via confidence level analysis; vii) if results for both cases in vi) are comparable, which means the disaggregation can be implemented without voltage, then connect disaggregation box with forecasting boxes and analyse joint confidence level. Further details will be described in the subsections.

1) Training

a) Weighting Factor (WF) and Voltage (V) Data Generation

To guarantee that all possibilities are considered and generated, the eight load categories are further divided into two parts, the dynamic part, including RCL, RWL, CTIM3 and QTIM3 categories, and the static part, including lighting, SMPS, rectifier and resistive load [15]. The dynamic part varies gradually from 0% to 100% with a 5% increase step, and the static part correspondingly varies with the dynamic part, decreasing from 100% to 0% with a 5% step. There are 21 possibilities of the dynamic-static combinations. For each possibility, the weighting factors (WFs) are generated randomly for different load categories within corresponding parts using Monte Carlo simulation. For example, for a 30% dynamic part and 70% static part combination, the WFs of different motor loads which make up the dynamic part are generated from 0% to 30%, and the WFs for all the other static loads which make up the static part are generated from 0% to 70%. The sum of WFs for all loads in each part remains unchanged, and all WFs generated are ensured

positive. The number of weighting factors generated for each dynamic-static combination is recorded as N_W.

As the power system bus voltages (under normal operation) generally vary from 0.9 p.u to 1.1 p.u and considering potential margins in extreme cases, the voltage range selected in this study is [0.85 p.u, 1.15 p.u]. Using Monte Carlo simulation, voltages ranging from 0.85 p.u to 1.15 p.u are generated randomly via uniform distribution to guarantee that all voltages are generated for training with equal probability. The number of voltage samples is recorded as N_V.

b) All combinations of WF and V

After random *WF* and *V* are generated using Monte Carlo simulation, all possible combinations of *WF* and *V* are obtained to generate the ANN inputs. As a result, the total number of such *WF-V* combinations is $21 \times N_W \times N_V$.

c) ANN Input and Target

For each *WF-V* combination, total P and Q at the bulk supply point are derived from (5), and they are regarded as RMS P&Q&V measurement from the supply point. For individual load categories in (5), P_i and Q_i under different voltages are calculated from the exponent-voltage relationship shown in Fig.3, (4) and (2). The inputs of ANN in the training process are total load real power P_{Agg}, total load reactive power Q_{Agg}, and supply voltage V (if available) at the supply point, defined as an input matrix ***PTRN*** shown as (6). The targets of ANN are corresponding weighting factors adopted to derive aggregate P and Q, defined as a target matrix ***TTRN*** shown as (7), where $w_{i,j}$ is the weighting factor of load category i for the j^{th} voltage-weighting factor combination, $1 \le i \le 8$, $1 \le j \le 21 \times N_W \times N_V$. All data in the input matrix and the target matrix are in p.u. values. In reality, it is usually not possible to predict every 30 *min* voltages. Therefore, in order to decide whether the disaggregation box can work without voltages, it is necessary to train and validate cases when the voltage is both available (Case 1) and unavailable (Case 2). In Case 2, the inputs for ANN are only P_{Agg} and Q_{Agg}, and the third row of (6) is removed.

$$\boldsymbol{PTRN} = \begin{bmatrix} P_{Agg,1} & \cdots\cdots & P_{Agg,21\times N_W\times N_V} \\ Q_{Agg,1} & \cdots\cdots & Q_{Agg,21\times N_W\times N_V} \\ V_1 & \cdots\cdots & V_{21\times N_W\times N_V} \end{bmatrix} \quad (6)$$

$$\boldsymbol{TTRN} = \begin{bmatrix} w_{1,1} & \cdots\cdots & w_{1,21\times N_W\times N_V} \\ \vdots \quad \vdots & w_{i,j} & \vdots \\ w_{8,1} & \cdots\cdots & w_{8,21\times N_W\times N_V} \end{bmatrix} \quad (7)$$

d) ANN Parameter Settings and Training

ANN main parameter setting includes hidden layer size setting and transfer functions setting [10], other parameters are configured as MATLAB default value because their effects are not as significant as hidden layer size and transfer functions [10]. The hidden layer size is defined as the number of neurons in the hidden layer, and is configured as the nearest integration to the estimation of (8) [20], where n is the number of neurons in the hidden layer, N is the number of the training pairs, and d is the input dimension. Log-sigmoid (*logsig*) and tan-sigmoid (*tansig*) are selected as the transfer function (TF) of the hidden layer and the output layer respectively to guarantee that the outputs of the ANN (weighting factors) fall between 0 and 1 [10].

$$n = \sqrt{N/(dlnN)} \quad (8)$$

As the training process covers almost all combinations of voltage and weighting, once trained, the ANN can be applied to extract the load composition at any time of any day in the future. Therefore, the robustness and the accuracy of the training algorithm are more concerned than the processing time. Thus, instead of Levenberg-Marquardt Backpropagation (LMBP), which is more popular because of its fast processing speed, BRBP with high accuracy and high robustness is selected as the training algorithm in this study, despite its longer processing time than LMBP. The trained ANN captures the relationship among P, Q, V (if available) and the load compositions, and the relationship is saved for validation and further use.

2) Validation

a) Validation Data Generation

Similar process for training data generation as described in Section V\B\1)\a)-Section V\B\1)\c) applies to validation data. According to (6) and (7), the input and the target in the validation process can be written as an input matrix ***PTST*** and a target matrix ***TTST***. ***TTST*** is adopted as a 'standard' to evaluate the performance of the trained ANN.

b) Validation Process and Aggregate Error

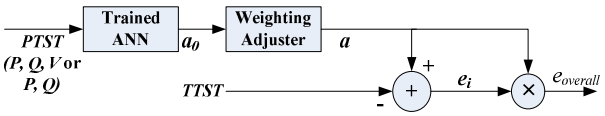

Fig. 4 Validation process block diagram

Fig.4 shows the validation process. Firstly, the input data ***PTST*** (P&Q&V or P&Q) passes the trained ANN to produce an output vector $\boldsymbol{a_0}$. $\boldsymbol{a_0}$ contains weighting factors of individual load categories computed by the trained ANN. As the computation process could induce computation error, the sum of each element inside $\boldsymbol{a_0}$ would probably deviate from 1. Therefore, a weighting adjuster is installed after the trained ANN to normalize $\boldsymbol{a_0}$, in order that the sum of the WFs is exactly equal to 1. The normalization is represented by (9), where a_i is the adjusted weighting factor for load category i, a_{0i} is the weighting factor for load category i before adjusting, N is the number of elements in vector $\boldsymbol{a}$ and $\boldsymbol{a_0}$. Thus, the weighting adjuster output, vector $\boldsymbol{a}$, is defined as the computed weighting factor.

$$a_i = \frac{a_{0i}}{\sum_{i=1}^{N} a_{0i}} \quad (9)$$

The output of the weighting adjuster is compared with the target ***TTST***, the initial weighting factors used to generate ***PTST***. The weighting factor error (WFE) of different individual load categories, Vector $\boldsymbol{e_j}$ shown in Fig.4, is obtained by taking the absolute difference between $\boldsymbol{a}$ and ***TTST***. To obtain the overall WFE ($e_{overall}$) (i.e. the load disaggregation error) of the disaggregation approach, an error aggregation approach is needed to combine individual WFEs into an aggregate WFE. The weighted average approach, represented by (10), is selected for error aggregation because

of its simplicity and higher accuracy than other more complicated approaches such as Bayesian approaches [13]. In (10), N is the total number of load categories, a_i is the computed weighting factor for load category i, e_i is the weighting factor estimation error for load category i in each error vector $\boldsymbol{e_j}$, $e_{overall}$ is the aggregate load disaggregation error (i.e. the overall WFE).

$$e_{overall} = \sum_{i=1}^{N} a_i e_i \tag{10}$$

c) Probabilistic Distribution and Confidence Level

As ***PTST*** contains large quantities of randomly generated validation data sets, WFEs calculated from (10) are probabilistically distributed. Therefore, PDF and CDF are used to obtain the probabilistic distribution and confidence levels (CL) of WFE intervals in order to assess the reliability of the disaggregation. PDF and CDF of WFEs in the disaggregation approach are notated as $f_D(e_D)$ and $F_D(e_D)$. They can also be interpreted as PDF and CDF of load composition forecasting error when the total load forecasting error has a 100% CL.

VI. Load Composition Forecasting Confidence Level and Probability Distributions

In the reality, the CL of specific total load forecasting error interval is not likely to reach 100% under most circumstances. Thus, the actual CL of load composition forecasting error, which is the joint CL of total load forecasting error and WFE, is lower than CL of WFE. Because the forecasting process and the disaggregation process are independent, the joint CL is the product of the CL (read from CDF) of total load forecasting error and WFE, shown as (11). The meaning of CL and CDF will be explained in more detail with examples in later sections. A similar relationship applies to joint PDF $f_{FD}(e_F, e_D)$.

$$F_{FD}(e_F, e_D) = F_F(e_F)F_D(e_D) \tag{11}$$

VII. Simulation and Result Analysis

Data collected on 16 working days between 24/05/2010 and 18/06/2010 are used to illustrate the total load forecasting approach, 12 of them for training and 4 for validation. The forecasting process takes up to 5 sec. In disaggregation, there are 8400 training sets and 2100 validation sets. The training process of the disaggregation takes up to 20 min and the validation takes up to 1 sec.

A. Total Load Forecasting Result

Fig.5a) shows forecasted P demand against actual P demand. Fig.5b) shows the total P forecasting error in p.u. at every sampling point on the testing days. Similar plots for reactive power prediction are not shown due to space limitation. Both figures indicate that the developed forecasting black box can predict the load with high accuracy. Fig.5c) shows PDF and CDF of absolute error of total P demand forecasting produced by MATLAB function *ksdensity()*. PDF indicates that the most likely absolute forecasting error occurs at about 1%, and CDF indicates the confidence level under different forecasting error interval. For example, for a real power forecasting with error lower than 3%, the confidence level is about 80%. (Note: The negative values of forecasted absolute errors in following figures showing CDF and PDF plots appear due to MATLAB's PDF/CDF curve fitting algorithm. For example, the CDF plot in Fig. 5c) shows that the probability of absolute error caused by curve fitting being below zero is 4.4%, thus it does not affect prediction accuracy significantly.) Fig.6a) shows PDF and CDF of absolute total Q forecasting error, and Fig.6b) shows PDF and CDF of overall total load forecasting error, which is defined as the mean value of the absolute P and Q prediction error.

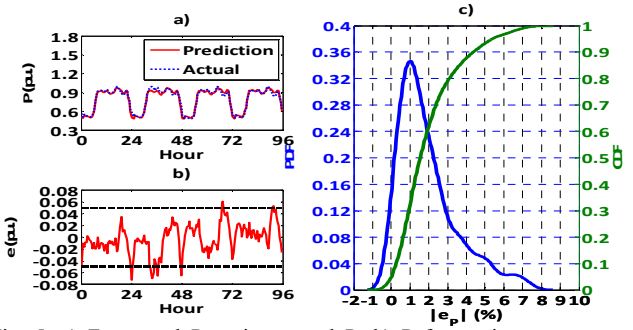

Fig. 5. a) Forecasted P against actual P; b) P forecasting error at every sampling point; c) PDF and CDF of absolute total P forecasting error

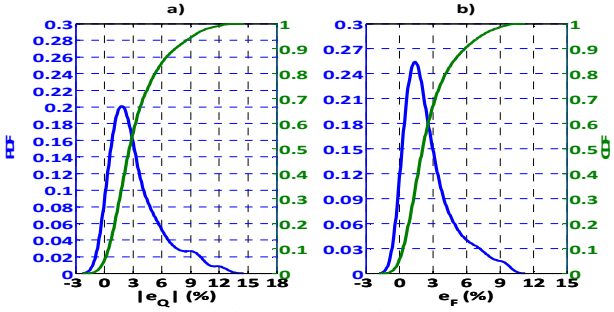

Fig. 6. a) PDF and CDF of absolute total Q forecasting error; b) PDF and CDF of absolute overall total load forecasting error

B. Disaggregation Result

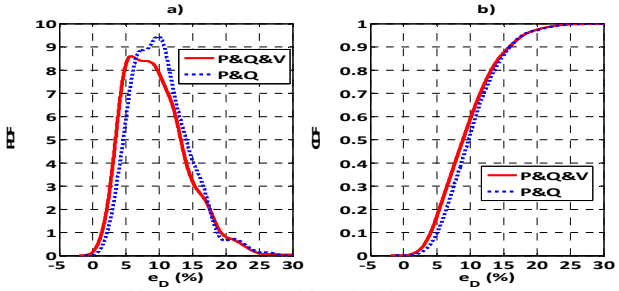

Fig. 7. a) PDF, and b) CDF of WFE with and without voltage

Fig.7 shows PDFs and CDFs of WFE in both cases when voltage is available (P&Q&V, Case 1) and absent (P&Q, Case 2). Although the 'most likely' disaggregation errors are different (i.e. 5% for Case 1 and 10% for Case 2), weighting factor error for both cases fall in the same range and have similar distribution. Two CDFs shows that the confidence levels for both cases under any WFE interval are very close, although Case 2 has a slightly lower confidence level than Case 1 does under the same WFE interval. In other words, in

the disaggregation process, the effect of the voltage is much less pronounced than aggregate load characteristics (i.e. P&Q). Therefore, the disaggregation process can be implemented without voltage measurement, and the disaggregation black box could be integrated with the forecasting boxes.

C. Load Composition Forecasting Result

Fig.8a) shows PDF of load composition forecasting error when CL of total load forecasting error is less than 100%. From Fig.8a), it can be seen that the most likely load composition forecasting error (e_D) is about 10% if the total load forecasting error (e_F) is about 1.2%, which matches the result shown in Fig.6 and Fig.7. Fig.8b) provides the confidence level (CL) of load composition forecasting error when CL of total load forecasting error is less than 100%. For example, for a load composition forecasting error (e_D) lower than 15%, if the total load forecasting error (e_F) has an 100% CL, then according to Fig.7b), the CL for the load composition forecasting in this case (i.e. CL for overall WFE) is approximately 90%. While, if the total load forecasting error is lower than 6%, which has an approximately 90% CL according to Fig.6b), then the CL of the load composition forecasting becomes 90%×90%=81%. The point which can represent this group of information in the order of (e_D, e_F, F_{FD}) is the Point (15, 6, 0.81) on the surface plotted in Fig.8b).

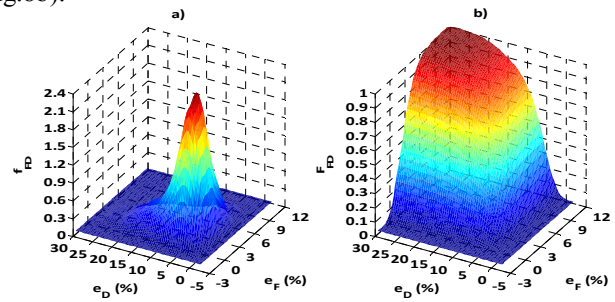

Fig. 8. a) PDF, and b) CDF of load composition forecasting error when total load forecasting error is less than 100%

VIII. CONCLUSIONS

An ANN based framework for developing a black box forecasting system for load composition forecasting is proposed in this paper. The load composition forecasting approach makes use of the developed total load forecasting techniques and the voltage dependent characteristics of the aggregate load at the bulk supply point to establish all three black boxes. Uncertainty in total load forecasting can reduce the confidence level of load composition forecasting, which highlights the importance of load forecasting accuracy. With the approach developed in this study, using measured real power, reactive power and forecasted weather data, it is possible to predict the percentage of different load categories (i.e. induction motors, lighting etc.) in advance, with forecasting error typically less than 10%.

The proposed approach will contribute to prediction of dynamic load response to voltage disturbances, which will benefit power system stability studies and close to real time control. Furthermore, it will inform operators and customers of the energy distribution in advance, inform demand side management decisions and provide suggestions for electricity price regulation. The methodology will also contribute to efficient renewable energy source (RES) integration in distribution networks so that not only the generation of RES can be fully utilized, but also the whole power system could operate more securely and economically.

REFERENCES

[1] J. W. Taylor and R. Buizza, "Neural network load forecasting with weather ensemble predictions," *IEEE Transactions on Power Systems,* vol. 17, pp. 626-632, 2002.

[2] M. Mordjaoui and B. Boudjema, "Forecasting and modelling electricity demand using Anfis predictor," *Journal of Mathematics and Statistics,* vol. 7, pp. 275-281, 2011.

[3] J. N. Fidalgo and J. A. Pecas Lopes, "Forecasting active and reactive power at substations' transformers," in *Power Tech Conference Proceedings, 2003 IEEE Bologna*, 2003, p. 6 pp. Vol.1.

[4] A. K. Bhatt, P. Solanki, A. Bhatt, and R. Cherukuri, "A fast and efficient back propagation algorithm to forecast active and reactive power drawn by various capacity Induction Motors," in *Circuits, Power and Computing Technologies (ICCPCT), 2013 International Conference on*, 2013, pp. 553-557.

[5] Intertek, "R66141 Household Electricity Survey_A study of domestic electrical product usage," 2012.

[6] D. R. Sagi, S. J. Ranade, and A. Ellis, "Evaluation of a load composition estimation method using synthetic data," in *Proceedings of the 37th Annual North American Power Symposium, 2005.*, 2005, pp. 582-588.

[7] M. Figueiredo, A. de Almeida, and B. Ribeiro, "Home electrical signal disaggregation for non-intrusive load monitoring (NILM) systems," *Neurocomputing,* vol. 96, pp. 66-73, 2012.

[8] L. Jian, S. Ng, G. Kendall, and J. Cheng, "Load Signature Study-Part I: Basic Concept, Structure, and Methodology," *IEEE Transactions on Power Delivery,* vol. 25, pp. 551-560, 2010.

[9] L. Jian, S. K. K. Ng, G. Kendall, and J. W. M. Cheng, "Load Signature Study-Part II: Disaggregation Framework, Simulation, and Applications," *IEEE Transactions on Power Delivery,* vol. 25, pp. 561-569, 2010.

[10] H. Demuth, M. Beale, and M. Hagan, "MATLAB Neural network tookbox user's guide," ed, 2009.

[11] K. Gurney, *An introduction to neural network*: UCL Press, 1997.

[12] Weather History @ Weather.org [Online]. Available: http://weather.org/weatherorg_records_and_averages.htm

[13] R. T. Clemen and R. L. Winkler, "Combining probability distributions from experts in risk analysis," *Risk Analysis,* vol. 19, pp. 187-203, 1999.

[14] J. V. Milanovic and I. A. Hiskens, "Effects of load dynamics on power system damping," *Power Systems, IEEE Transactions on,* vol. 10, pp. 1022-1028, 1995.

[15] CIGRE, "Modelling and aggregation of loads in flexible power networks," Working Group C4.605, Rep. 5, May. 2012.

[16] C. Cresswell, S. Djokic, K. Ochije, and E. Macpherson, "Modelling of Non-Linear Electronic Loads for Power System Studies: A Qualitative Approach," presented at the 19th Int. Conf. on Electricity Distribution CIRED 2007, 2007.

[17] C. Cresswell and S. Djokic, "Steady-state models of low energy consumption light sources," presented at the 16th Power Systems Computation Conference PSCC 2008, 2008.

[18] C. Cresswell and S. Djokic, "Representation of directly connected and drive-controlled induction motors. Part 2: Three-phase load models," in *Electrical Machines, 2008. ICEM 2008. 18th International Conference on*, 2008, pp. 1-6.

[19] C. Cresswell and S. Djokic, "Representation of directly connected and drive-controlled induction motors. Part 1: Single-phase load models," in *Electrical Machines, 2008. ICEM 2008. 18th International Conference on*, 2008, pp. 1-6.

[20] S. Xu and L. Chen, "A novel approach for determining the optimal number of hidden layer neurons for FNN's and its application in data mining," in *5th ICITA*, 2008, pp. 683-686.